# Evaluation of Plasma Clearance by Synthesis of Continuous Infusion: Principles and Use

Norman J. Chonacky and F. Deaver Thomas

*Division of Nuclear Medicine, Department of Radiology, SUNY Health Science Center at Syracuse, Syracuse, New York*

There is a technique of engineering analysis which can be described as "impulse synthesis" which uses the observational data of a system's response to a single sharp blow in order to predict its response to a steady force. This same technique has been applied to the calculation of in situ drug levels and for calculating plasma clearance values. The purpose of this paper is to elucidate the principles of this calculation technique and to critically assess its application to plasma clearance studies. We begin by tracing the history of the measurement of renal clearance of plasma. We then proceed to exposit the relevant principles of the synthesis technique. Finally, we report the results of our application of this technique to the analysis of simulated data in a manner intended to be of use to clinicians who might wish to consider employing the technique.

**J Nucl Med 27:1611–1622, 1986**

Wooten and Sanderson have applied the technique of impulse synthesis to the calculation of in situ drug levels (*1*), and most recently Veale has suggested it for calculating plasma clearance levels (*2*). In this method, we administer a single injection of a radioactive substituent with activity ($N_o$) into the circulatory system and we monitor the progress in the plasma of both mixing and clearance of this tracer by periodically drawing blood samples. The set of all such sample activities versus their time of extraction form a graph whose functional definition is

$$F[t] = (\text{activity/vol}) \qquad (1)$$

for each plasma sample drawn at a time (t) after injection of the tracer at t = 0.

We usually normalize the set of these values (F[t]) to the activity ($N_o$) of the injection to form a normalized, single-injection plasma response function (P[t]) in the following manner:

$$\begin{aligned} P[t] &= (1/N_o)\, F[t] \\ &= (\text{activity}/N_o)/\text{vol} \\ &= (\text{fractional activity/vol}). \end{aligned} \qquad (2)$$

This function (P[t]), a merely rescaled form of (F[t]), summarizes the primary experimental data of a single-injection plasma clearance experiment. Typically such a function, interpolated and smoothed of experimental fluctuations, looks like that depicted in Fig. 1.

A most important physiological parameter is the clearance value (C) for the given injected substituent. This value is related to the rate of substituent removal (R) by the kidneys, from the local concentration (K) in the plasma there, by the following equation which is definitive for (C):

$$R[t] = K[t]\, C. \qquad (3)$$

This equation assumes that the removal rate is always simply proportional to the instantaneous local concentration. Notice that if (K) is measured in units of activity per volume, and (R) in units of activity per time, then the clearance (C) must be a volume per time.

There are basic practical problems with trying to use Eq. (3) to evaluate the clearance (C). The instantaneous removal rate (R) of tracer substituent from the kidney is not practically measurable. Moreover, in the dynamic situation the tracer concentration throughout the entire plasma pool is undoubtedly not uniform (*6*). Thus, if you sample the concentration (F) at one point in the body, you cannot simply infer at any instant of time that

$$K[t] = F[t] = (N_o)\, P[t]. \qquad (4)$$

If you could both measure (R) and infer (K) from measurements (F), then you could use them with Eq.

Received June 19, 1985; revision accepted Mar. 17, 1986.

For reprints contact: F. Deaver Thomas, Div. of Nuclear Medicine, Dept. of Radiology, SUNY Health Science Center at Syracuse, Syracuse, NY 13210.

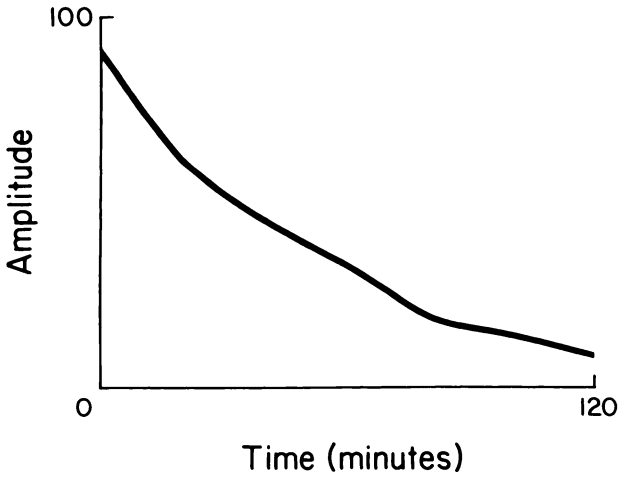


**FIGURE 1**
Plasma activity response to a single injection at t = o

(3) to experimentally evaluate (C). In fact, except in one special case which we present later, any attempt to relate the removal rate (R[t]) to the experimentally measurable (F[t]) must necessarily make model-dependent assumptions about the mixing of the tracer substituent into the extracellular spaces. Since the kidney clearance is but one of a composite of processes which affect the substituent concentration in the plasma and because there are several such processes, the information about clearance lies intertwined with that of mixing, within the function (F[t]). Our task is to extract it in evaluating (C).

Many methods have been developed to use the information of single-injection plasma response functions (P[t]) to evaluate the desired renal plasma clearance rate (C). Most of these deal directly with the function (F[t]). Some of these methods (*3*) are based upon empirical calibrations which connect a specific value ($F[t_{sp}]$) to the clearance rate. Others (*4–7*) attempt to use reasonable models of the clearance process to derive how the shape and size of a predicted, ideal response function relate to a given clearance rate. These ideal curves are then fitted to the actual functional form of (F[t]) to evaluate the clearance rate.

Both of these traditional approaches to the problem of clearance rate evaluation are burdened by the dynamics of the mixing and clearance processes. For any given injected substituent, the clearance process is complicated by mixing within the plasma and into the various extracellular fluid compartments accessible to that substituent (*6*). Each particular configuration of these various systemic compartments accessible to the substituent produces, in general, a different functional form for (P[t]) even when the clearance is the same. Thus, empirical calibration methods ought to anticipate all the various systemic types and generate a calibration factor for each. Modelling methods, on the other hand, must not only identify the relevant mixing processes but also must model the dynamics of each accurately.

In our experience, random experimental errors are also a significant problem in obtaining accurate results. Such effects are referred to as "noise" and the idealized, error-free values as "signal" in the vocabulary of the electrical engineer. In such terms our experimental method frequently suffers from a low "signal-to-noise ratio." Both of the traditional approaches to evaluating renal clearance from the single-injection response function are burdened by not having a natural way to average out these random experimental errors.

We would like to have a technique for evaluating renal clearance which does not rely upon empirical calibrations, which is not model dependent, and which suppresses the destabilizing influences of experimental noise upon the outcome. The impulse synthesis method which we are about to describe has these features.

**Fundamental Principles**

The simplicity of Eq. (3) tempts us to find a way to use it for determining the clearance value. Recall that experimental measurement of the instantaneous values (R[t]) generally is impractical. However, there is a condition in which one limiting value of (R[t]) can be readily determined. This condition is the steady state and the value ($R_e$) is that which is obtained from maintaining a continuous infusion of a substituent at a rate (I) until the plasma sample activity ($F_c[t]$) no longer depends upon time, having reached its asymptotic value, $(F_c)_e$. At this point the plasma system has come to equilibrium with the extracellular fluid, steady state has been achieved, and the renal removal rate has come to match the infusion rate. Thus,

$$I = R_e = \lim_{t \to \infty} \{R[t]\}. \qquad (5)$$

Notice that we have used the symbol ($F_c[t]$) above for the general response to a continuous infusion. In that *particular* limit of ($F_c$) which corresponds to the steady state, you *can* validly use a simple assertion such as Eq. (4):

$$K_e = (F_c)_e = (N_o)\,(P_c)_e. \qquad (6)$$

Although ($P_c[t]$) is still defined exactly in the manner of (P[t]) in Eq. (1), its analog in the single-injection case, its functional form will be quite different. In addition, strictly speaking, the factor ($N_o$) on the right of Eq. (6) has no meaning in the continuous infusion case, since we are using a steady, rather than one initial, injection. However, we retain this form and temporarily reinterpret ($N_o$) to be *any* arbitrary activity. We do this for reasons of computational convenience that will become apparent in our derivations below which relate the continuous infusion case to the single-injection case.

Using Eqs. (3), (4), (5), and (6) together:

$$I = (N_o)\,(P_c)_e\,C;$$

or, solving for (C):

$$C = \frac{I}{(N_o)(P_c)_e}. \quad (7)$$

This permits the evaluation of the clearance in terms of measurable quantities:

$I$ = continuous infusion rate (activity/time);

$(N_o)(P_c)_e = (F_c)_e$ = steady-state value (activity/vol) of plasma samples.

Although continuous infusion is a straightforward experimental procedure, it is not clinically sound; it may require lengthy administration of a considerable amount of radioactive material while the desired equilibration is taking place. The synthetic approach which we now describe extracts the clearance value from single-shot data even while it relies upon the logic of the continuous infusion method. Instead of actually performing the continuous infusion, we use a computer to simulate it. *In effect, the computer calculates what would be the system's response to a steady repetition of injections, basing its calculation on how the system responded to a single shot.* This approach utilizes the single-injection response (P[t]) as its sole source of experimental information. The reasoning behind this method of impulse synthesis follows.

Our first objective is to relate the continuous infusion response function ($P_c[t]$) to the single-shot response (P[t]). If the first single injection ($N_o$) at ($t = 0$) was followed by a second injection ($N_1$) some time ($t = t_1$) later, then the response of those combined injections would be,

$$P_s[t] = P[t] + (N_1/N_0)\, P[t - t_1]. \quad (8)$$

This sum, in effect, superimposes two graphs of the single-injection plasma response by adding to the original (P[t]) graph another one shifted by an amount ($t_1$) along the time axis and scaled with the relative strength of the second injection ($N_1/N_0$). These component graphs appear in Fig. 2, along with their sum graph ($P_s[t]$). The advantage of retaining the factored form of Eq. (6) now emerges. It permits us to scale the effects of subsequent injections to the first injection (or any other standard value we wish). Equation (8) retains the normalized quality of Eq. (2). This is reflected in the fact that $P_s[t]$ has the same physical units as P[t], the original single shot response; the coefficient ($N_1/N_0$) of the subsequent term in Eq. (7) appears conveniently as a unitless ratio or superposition weight.

We assert that a suitable generalization of ($P_s[t]$) can be used to predict the response function for continuous infusion ($P_c[t]$). The validity of such an assertion rests necessarily upon the truth of two conditions:

1). The plasma system response to the second injection is independent of the presence of the material from the first. (Property of *linearity.*)

2). The plasma system response at time ($t = 0$) is the same as at time ($t = t_1$), and all subsequent times. (Property of *stationarity.*)

These conditions are at the heart of the "impulse synthesis" method. In fact, the very concept of a characteristic clearance parameter (C) implicitly presumes a linear system. Questions of the validity of condition 1 are thus moot. The validity of condition 2, on the other hand, must always be considered on a case by case basis, and presents an essential limitation to the applicability of this method.

Suitable generalization requires that ($P_s[t]$) represent the response to an increasingly repetitive series of injections in order that

$$P_s[t] \rightarrow P_c[t].$$

Consider an infinite set of periodically spaced single "injections." To the extent that the time intervals ($\Delta t$) between them are "small" compared to the time for the system steady-state, the predictive plasma response should approach that expected from a continuous injection, again assuming that conditions 1 and 2 are physically justifiable.

To express in mathematical terms the logic of superimposing this sequence of response terms, we adopted the following notation. Let the generalization of any one of the terms in Eq. (8) be

$$\Delta P_j[t] = (\Delta N_j/N_o)\, P[t - t_j]. \quad (9)$$

Each ($\Delta P_j[t]$) is the response to the j-th injection ($\Delta N_j$), administered at time ($t_j$), where we have defined $t_{j=o} = 0$. Here again, as in Eq. (8), the weighting coefficients specify the relative contributions of each single-shot response to the superposition. Figure 3 shows the component and sum response graphs for the multiple, equal-injection, equal-interval case. It is analogous to Fig. 2 which depicts the two-component case. Proceeding to sum the expressions for the component functions, from Eq. (9) above:

$$\begin{aligned} P_s[t] &= \sum_j (\Delta P_j[t]) \\ &= \sum_j \{(\Delta N_j/N_o)\, P[t - t_j]\} \quad (10) \\ &= (1/N_o) * \sum_j \{(\Delta N_j)\, P[t - t_j]\}. \end{aligned}$$

Equation (10) lacks explicit reference to an infusion rate. The simulated, steady infusion rate ($I_s$) is that responsible for "producing" the response function ($P_s[t]$). ($I_s$) depends upon the size of the elemental injections ($\Delta N_j$) as well as upon the inter-injection time interval ($\Delta t$). In general,

$$I_s[t_j] = \Delta N_j/(t_{j+1} - t_j). \quad (11)$$

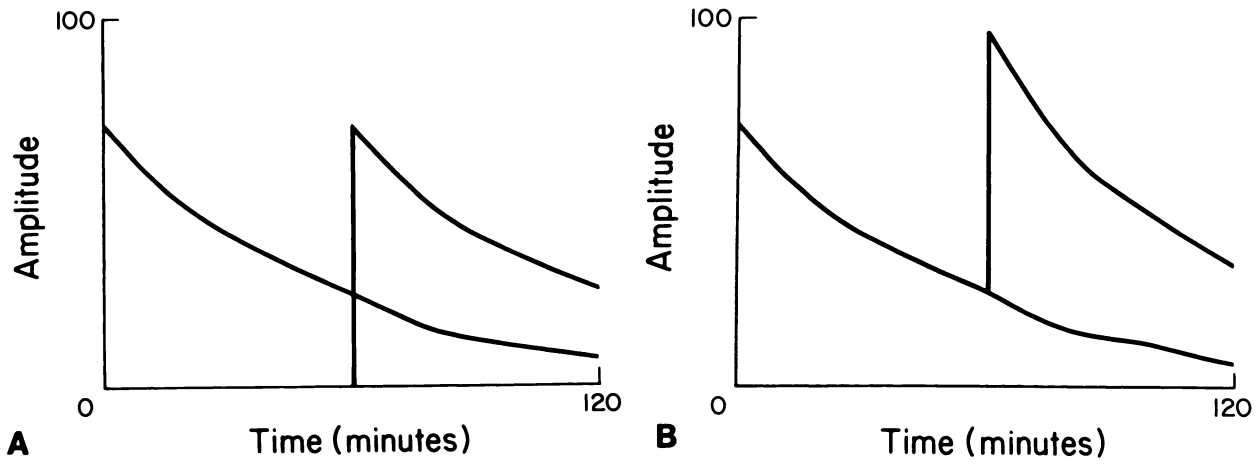


**FIGURE 2**
(A) Two single-injection plasma responses, shifted by 60 min, (B) Same two, shifted responses, added

In this derivation we restrict ourselves to consideration only of identical injection values

$$\Delta N_j = \Delta N$$

injected at identically-spaced times

$$(t_{j+1} - t_j) = \Delta t$$

so that the simulated, quasi-continuous infusion rate from Eq. (11) in this case reduces to a constant which can be expressed as

$$I_s = (\Delta N/\Delta t). \quad (12)$$

Under these conditions ($\Delta N_j$) may be factored from the sum in Eq. (10) as ($\Delta N$):

$$P_s[t] = (\Delta N/N_o) * \sum_j (P[t - t_j]). \quad (13)$$

This Eq. (13) is the proper generalization of Eq. (8) to the multiple injection case. Equations (12) and (13) may now be combined to yield:

$$P_s[t] = ((I_s * \Delta t)/N_o) * \sum_j (P[t - t_j]). \quad (14)$$

We assert that, in the limit of ($t \rightarrow 0$) and ($j \rightarrow \infty$), ($P_s[t] \rightarrow P_c[t]$) and ($I_s \rightarrow I$); i.e., the superposition approximates the actual plasma response which would be measured in the case of continuous infusion rate (I). Figure (4) shows a graphical attempt to depict this limiting case by replacing the explicit composite graph with a stylized envelope. The horizontal bars are the average values for the piecewise function segments. In the limit discussed, these pieces would coalesce to form a continuous curve (S[t]). This curve is the limiting sum on the right-hand side of Eq. (14) above.

$$S[t] = \lim_{\Delta t \to 0} \{\sum_j P[t - t_j]\}. \quad (15)$$

This new function (S[t]) is simply the sum of the superimposed graphs. In the limiting case being dis-

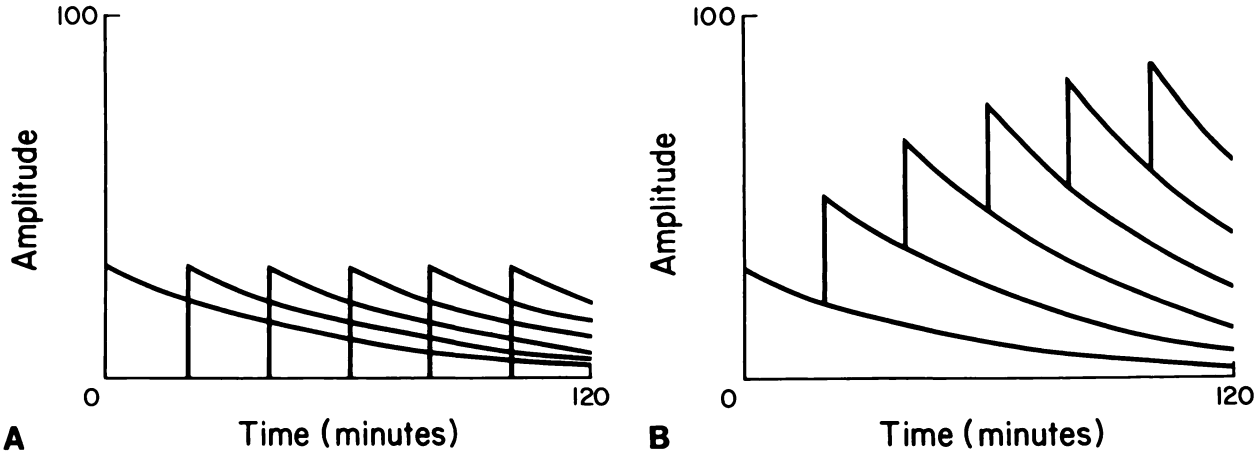


**FIGURE 3**
(A) Six single-injection plasma responses, shifted by 20 min, (B) Same six, shifted responses, added

cussed, the left-hand side of Eq. (14) becomes

$$P_c[t] \equiv \lim_{\Delta t \to 0} \{P_s[t]\}.$$

Combining this with Eq. (15) we obtain

$$P_c[t] = \{(I * \Delta t)/N_o\} * S[t]. \quad (16)$$

This relation holds for every instant of time (t). In particular it holds in the asymptotic equilibrium limit, in which case Eq. (16) becomes

$$(P_c)_e = \{(I * \Delta t)/N_o\} * (S_e). \quad (17)$$

Equation (17) involves steady-state quantities [c.f. Eq. (7)]. From Eq. (15) (and Fig. 4), we reason that the graph (S[t]) is the limiting superposition of all the mutually displaced, single-shot graphs (P[t]). ($S_e$) is the asymptotic value:

$$S_e \equiv \lim_{t \to \infty} \{S[t]\}.$$

We now finally see how to evaluate (C) in terms of directly measurable, given, and calculable quantities. Equation (7) becomes

$$\begin{aligned} C &= (I/N_o) * (1/(P_c)_e) \\ &= (I/N_o) * (N_o/(I * \Delta t * S_e)) \quad (18) \\ &= 1/(\Delta t * S_e). \end{aligned}$$

Thus, the (superposition) sum graph's asymptotic value ($S_e$), and the value for the time displacement interval ($\Delta t$) used in forming that sum, are sufficient to evaluate the clearance (C) from the single-shot information. The arbitrary activity value ($N_o$) has turned out to be, as promised, a conceptual/notational convenience which cancels out in the end result.

We have pointed out the difficulties inherent in trying to connect the plasma substituent concentration in the kidney to its removal rate in the dynamic (non steady-state) case. We have derived that connection for a steady-state situation in which an iterative calculation technique simulates the physical administration of a continuous substituent injection. We are now prepared to discuss the employment of this method of analysis for the evaluation of clearance rate (C) from the single injection data only.

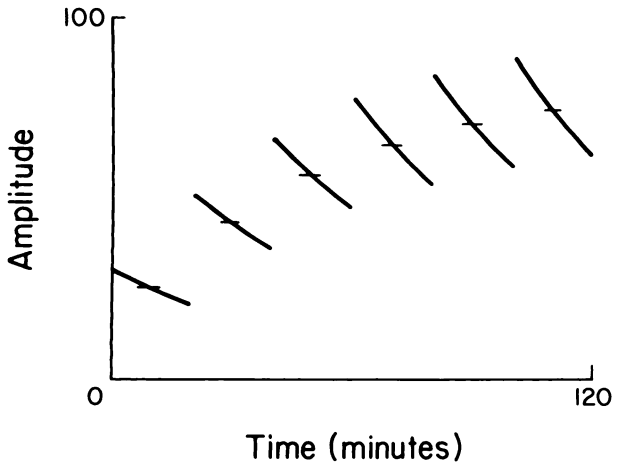


**FIGURE 4**
Same six shifted and added components as shown in Fig. 3, with average values (for each six intervals) depicted by horizontal bars

**Development and Testing of the Algorithm**

In this section we discuss the manner of our testing of the computational algorithm which we designed to calculate the superposition of single-shot response curves resulting in the sum curve (S[t]) as defined in Eq. (15). There are some fundamental practical difficulties which prevent us from employing Eqs. (15) and (18), exactly as they stand, for this purpose. Our discussion briefly enumerates these difficulties and states our design decisions for dealing with them. Since our approach to developing the algorithm was experimental but the purpose of this paper is practical application, we state only the results of our experiments as they affect intelligent use of the algorithm. A structured-design outline of the computer program embodying the algorithm which we used is contained in the Appendix.

First, the plasma sampling experimental data are usually incomplete because the time span (T) of experimental sampling is less than that required for the single-shot response to vanish. This we call the TRUNCATION problem. We deal with it by providing an initial "priming" injection, i.e., increased coefficient ($\Delta N_o$) for the first term in the synthesis sum, which permits us to compensate to a certain extent for the missing data. Our criterion for achievement of the steady state is that the slope ($\Delta S[t]/\Delta t$), averaged over a suitable terminal portion of that curve, vanishes.

Second, the data samples are always subject to certain random measurement errors. These can result in variation of the measured values which are a considerable fraction (typically 5–10%) from their "ideal" noise-free values. This we call the NOISE problem. We deal with it by providing optional smoothing. This is in addition to the natural smoothing inherent in our integrative (superposition) approach. The explicit smoothing is made optional because it can contribute some systematic error of its own, under certain circumstances.

Third, the data samples are discrete. Typically about 6–8 plasma samples are drawn per single-injection study. The logic of our method (c.f. Eq. (15)) requires that we use a shift-and-add time interval ($\Delta t$) as "small" as possible. This requirement conflicts with the finite sample time intervals, a situation which we call the SAMPLING problem. We deal with this by interpolating between the sampled values and by affording the user a choice of value for ($\Delta t$). The freedom of this choice is limited somewhat by the fundatmental limit

in information concomitant with the finite number of data samples.

We address several questions in assessing the performance of our algorithm in evaluating renal clearance of a plasma system.

1) How *accurate* is it; that is, does it yield the correct value for the actual system clearance?

2) How *precise* is it; that is, how close an agreement is there among its results when applied to different data sample sets drawn from the same system?

3) How *robust* is it; that is, does it perform satisfactorily (according to the above criteria) for a wide range of system values, or are there "bad cases"?

4) How *reliable* is it; that is, how changeable are the results from using it in several different ways (different choices for operating parameters ($\Delta t$), priming injection, optional smoothing, etc.) on the same input data set?

We believe that it is especially important to actually test the algorithm in controlled circumstances for these performance qualities. This follows because the connection between the form of the data and the form of the resultant superposition solution function is so far from obvious that we lack the usual intuitive clues as to how well we are doing. Thus, you cannot rely on intuition to be a very helpful guide in suggesting which choices for operating parameters or which types of input data cause ill-conditioned behavior which might compromise the validity of the computational result. Accordingly, we prepared a considerable number of simulated data sets for which we knew the clearance values and noise figures; we carried out an extensive series of evaluative tests using them. From the results of these test studies we were able to scrutinize the effects upon algorithm performance both due to choices in its design options and due to selections for its operating parameters.

In order to interpret the test results in terms of insights into actual physiological cases you must know how the simulated data sets, constructed for use in the studies, are related to the model system whose behavior they were designed to simulate. This model is depicted schematically in Fig. 5. It consists of two compartments separated by a diffusion-controlled membrane. One of these compartments is the plasma volume ($V_1$) and the other is the extracellular fluid volume ($V_2$). The permeability of the separating membrane is ($C_2$) and the effective permeability of the kidney which clears ($V_1$) is ($C_1$). ($C_1$) is equivalent to the clearance (C) used earlier; hence, we use the same notation here. The general form for all these simulated data sets is

$$\frac{N[t]}{(V_1)\,(N_o)} = Ae^{-t/a} + Be^{-t/b}. \qquad (19)$$

Thus, the parameters ($V_1$, $C_1$, $V_2$, $C_2$) must be related to the parameters (A, a, B, b) in Eq. (19) (*8*).

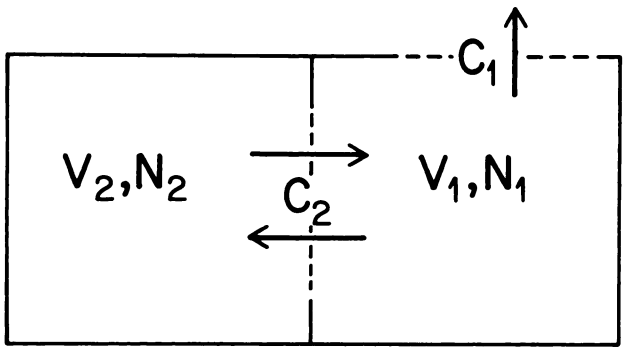


**FIGURE 5**
Schematic diagram of two-component model system. $V_1$ = volume of plasma; $V_2$ = volume of extracellular fluid; $C_1$ = permeability of clearance "membrane"; $C_2$ = permeability of plasma/extracellular exchange "membrane"

In conjunction with this system, there are two characteristic times: T′ and T″. These times are related to two physical processes. (T′) is the characteristic time for decay of the activity by clearance from the plasma volume in the ideal single compartment system. Therefore (1/T′) is the characteristic rate for the activity to be cleared from the plasma compartment by the kidney. And (T″) is the characteristic time for equilibration of the activity between the plasma volume and the extracellular volume in the hypothetical system which has no kidney clearance. Therefore (1/T″) is the characteristic rate for the activity to diffuse across the two-compartment membrane. Moreover, these time values are completely determined by ($V_1$, $C_1$, $V_2$, $C_2$). In particular,

$$T' = V_1/C_1;$$

$$T'' = V_2/C_2.$$

Then, given any particular value for (T′), the other (T″) has its value fixed by the permeability ratios ($C_2/C_1 \equiv R_c$) and volume ratio ($V_2/V_1 \equiv R_v$). Thus the simulated system is completely specified by the three quantities: (T′, $R_c$, $R_v$). These shall be our independent variables. Accordingly, in reporting each of our test results we shall specify the model system used by specifying these three quantities. Recall that ($C_1 \equiv C$), the desired clearance value. In testing we may fix ($V_1 = 1$) without loss of generality. In that case ($C = 1/T'$); i.e., the value for the clearance of the simulated system is numerically equal to the reciprocal of the value of (T′) chosen in constructing that simulation. This relation connects the "idealized" clearance value of any particular simulation to one of the characteristic parameters of that simulation. These facts will help you to interpret the results of our tests which use simulated data.

We point out here that our simulation studies routinely used several combinations of values ($R_v$ and $R_c$). The physiological meaning of larger values for ($R_v$) i.e., ($V_2 \gg V_1$) has to do with edema. In edematous patients,

($R_v = 5$), or even greater. The physiological meaning of values of ($R_c$) has to do with relative accessibility of the injected substituent to the extracellular ($C_2 \gg C_1$) fluid. Values of ($R_c > 1$) means that leakage dominates; a value ($R_c = 1$) means that the clearance and the leakage to extracellular fluid are comparably effective processes.

These simulation studies were carried out in a variety of noise and signal sampling environments. For example, our experience shows that noise levels of (5–10%) of signal levels are usual in clinical data. In the testing process, when evaluating the effects of noise, we separately introduce (10% and 20%) RMS random Gaussian errors in the simulated data just to be on the safe side, and evaluate the performance for each. As another sample, for the characteristic clearance time (T′) in the simulated data we use several values, each a fraction of the sampling time span (T) which was T = 120 min in all cases. Thus, in the testing process we can evaluate the algorithm performance for various degrees of completeness of the input information. Specifically: T′ = T/4; T′ = T/2; and T′ = T, corresponding to progressively *less* complete input information.

## RESULTS

Preliminary testing helped us to make certain basic algorithm design decisions. These decisions address several problems already described. Two of these decisions deal with the *truncation* problem:

1) The time interval used for averaging the slope ($\Delta S[t]/\Delta t$) in the determination of the steady state condition {i.e., ($\Delta S[T]/\Delta t$)} was selected as [$3T/4 < t <= T$];

2) Every terminal value (S[T]) of the (superposition) sum function turned out to be very nearly a linear function of the terminal slope average value, over a wide range of choices for the initial component amplitude ($\Delta N_o$). Thus we do not have to resort to iteratively fishing for the particular value of ($\Delta N_o$) which results in a zero terminal slope {($\Delta S[T]/\Delta t$) = 0}, in order to evaluate ($S_e$). Instead, we make the determination of ($S_e$ = S[T]) by linearly extrapolating {S[T] vs. ($\Delta S[T]/\Delta t$)} to the point {($\Delta S[T]/\Delta t$) = 0)}. Since the extrapolation is linear, we need use only two pairs of computed values {S[T], ($\Delta S[T]/\Delta t$)}. Usually we employ those pairs resulting from using "priming injections" ($\Delta N_o = 1$) and ($\Delta N_o = 2$).

One of these decisions deals with the *noise* problem:

3) The smoothing operation was left as a user option and its consequences were evaluated at various points in the test series.

And one of these decisions deals with the *noise* and *sampling* problems:

4) The effect of time-shift value ($\Delta t$) upon the determined steady state values was sufficiently weak (Table 1) that a fixed value of ($\Delta t = T/24$) was arbitrarily adopted. This generously fulfilled the "optimal" noise averaging condition that the time-shift be about one-fourth the average sampling interval.

In all of the subsequent systematic tests, the simulated input data were specified at a set of canonical sample time points, selected because they are typical of the majority of the experimental protocols used in our laboratory studies. These sample points were always: t = 10, 20, 40, 60, 80, 100, and 120 min. The sampling time span was always T = 120 min.

We carried out one group of simulation tests to evaluate the accuracy of the algorithm. We explored the degree to which it is able to extract the proper simulation design value of clearance (C) under various conditions of completeness for the sampling. Each simulated data set was created using one of three values for its idealized, design clearance time (T′ = 30, 60, or 120 min), even while the sampling time span was fixed at (T = 120 min). Thus the input samples of the simulated data always spanned, respectively, four, two, or one

**TABLE 1**
Equilibrium Values ($S_e$*$\Delta t$) for Selected Data Sets*

| | | | | | | Δt (min) | | | | | | | |
|---|---|---|---|---|---|---|---|---|---|---|---|---|---|
| T† | T′‡ | $C_2/C_1$ | $V_2/V_1$ | Wtg§ | Noise | 0.2 | 0.5 | 1 | 2 | 4 | 5 | 10 | 20 |
| 60 | 30 | 5 | 1 | f(1) | 0 | 30.0 | 29.7 | 29.8 | 29.8 | 29.8 | 29.7 | 29.7 | 29.7 |
| 60 | 30 | 5 | 1 | f(1) | 5% | 34.4 | 35.3 | 38.2 | 43.2 | 41.6 | 34.2 | 30.6 | 30.3 |
| 60 | 30 | 5 | 1 | f(2) | 0 | 30.0 | 29.7 | 29.8 | 29.7 | 29.8 | 29.7 | 29.8 | 29.7 |
| 60 | 30 | 5 | 1 | f(2) | 5% | | 28.2 | 28.5 | 28.8 | 29.7 | 31.0 | 34.3 | 33.1 |
| 120 | 30 | .5 | 10 | f(3) | 0 | | | 21.5 | 21.7 | | 21.5 | 21.3 | 21.3 |
| 120 | 120 | .5 | 10 | f(3) | 0 | | | 81.2 | 81.6 | | 81.3 | 80.9 | 81.2 |

*Resulting from calculations using various time-shift increments. The effects from use of several weighting functions for evaluating terminal slope are also shown. We eventually adopted f(2) which is described in the text.

†T = Sampling span (min).

‡T′ = Characteristic clearance time (min), to be compared with ($S_e$*$\Delta t$) in each case.

§Wtg = Weighting.

No data smoothing.

times the period (T′), which is the characteristic clearance time. These cases represent progressively *less* completeness of the sampled information. In this manner we explored the effects of a whole range of TRUNCATION conditions of the input data on the accuracy of our method.

We also explored the degree of algorithm robustness by assessing its accuracy under various conditions of competition for the injected substituent between the kidney and the extracellular fluid. Each simulated data set uses a different combination of compartment volumes, {plasma ($V_1$) and extracellular ($V_2$)} and transfer permeabilities, {plasma-kidney ($C_1$) and plasma-extracellular ($C_2$)}. Throughout, we used the following various systematic combinations as canonical values:

$$[R_v \equiv V_2/V_1 = 1, 4, 10] \text{ and } [R_c \equiv C_2/C_1 = 0.2, 0.5, 1.0, 5.0].$$

Recall here that the relevant characteristic times of the competitive diffusion processes for the injected activity are the respective ratios:

$$[(V_1/C_1) = T'] \text{ and } [(V_2/C_2) = T''].$$

Also remember that we have contrived our simulated data so that there is a numerical equality:

$$|T'| = |1/C_1| \equiv |1/C|.$$

Combining these facts with Eq. (18) makes interpretation of the results in Table 2 easier. The degree of success of the algorithm in avoiding systematic error is measured by the degree of agreement between:

$(\Delta t)\,(S_c)$ ..... (computed); and

$(T')$ ..... (simulated).

Figures 6A, B, and C show summative graphical results of the kind listed as numerical examples in Table 2. The contours in Fig. 6 represent fixed levels of systematic error encountered in the observed calculation result {$(\Delta t)\,(S_c)$} as compared with the expected value (T′) for various combinations of ratios ($R_v$ and $R_c$). Each of these three contour graphs belongs to a different value of characteristic clearance time [$T' = (V_1/C_1)$]. You can see from intercomparing all three figures that the systematic error is least when the input function is most completely sampled (i.e., $T' \ll 120$ min). The systematic error is generally greater when the intrinsic clearance time (T′) approaches the sampling time span (T = 120 min) (i.e., when the input function is least completely sampled of all the test cases).

A normative physiological value for the extracellular/plasma volume ratio is [(V2/V1) ≅ 4]. Following this ordinal line on each of the three systematic error graphs reveals that these errors vary as the intercompartment permeability ratio varies over the range [$0.2 \leq (C_2/C_1) \Leftarrow 5.0$]. {N.B., equilibration between compartments is *faster* as the ratio ($C_2/C_1$) is larger.} Generally there is a maximum error at some point along this line. For the case where (T′ = 30 min), this maximum (error ≅ 20%) occurs at [$(C_2/C_1) = 0.4$]. For the case (T′ = 120 min), this maximum (error ≅ 50%) occurs at [$(C_2/C_1) = 2.0$]. One conclusion which you might draw from these results is that the algorithm becomes more vulnerable to the competitive effects of the extracellular fluid as the degree of sample completeness diminishes.

Subsequently, for each of the above simulated system conditions, we created several different data realizations having a given, fixed (percentage fractional random error. For each conditional set we produced two such sets of realizations, each using one of two levels of RMS error: 10% and 20%. These levels are in a range which our experience indicates is typical for random experimental error. In real data these error fluctuations are

**TABLE 2**
**Equilibrium and Advantage Values for Selected Simulated Noiseless Data Sets***

| Conditions: Wgt = f(2), no noise | | | | | | | | |
|---|---|---|---|---|---|---|---|---|
| | | | Without smoothing | | With smoothing | | | |
| T′ (min) | $(C_2/C_1)$ | $(V_2/V_1)$ | $(\Delta t)(S_e)$ | %err | $(\Delta t)(S_e)$ | %err | CA | AA |
| 30 | 0.2 | 1.0 | 27.8 | −7 | 26.1 | −12 | −0.54 | −5.2 |
| 30 | 0.5 | 1.0 | 29.4 | −2 | 28.8 | −4 | −0.71 | −2.1 |
| 30 | 1.0 | 1.0 | 29.9 | 0 | 30.2 | +1 | −3.45 | −1.30 |
| 30 | 5.0 | 1.0 | 28.9 | −4 | 30.1 | 0 | +3.38 | +7.3 |
| 30 | 0.2 | 4.0 | 25.9 | −14 | 24.1 | −20 | −0.36 | −6.1 |
| 30 | 0.5 | 4.0 | 24.2 | −19 | 22.4 | −25 | −0.28 | −6.0 |
| 30 | 1.0 | 4.0 | 28.0 | −7 | 27.0 | −10 | −0.36 | −3.0 |
| 30 | 5.0 | 4.0 | 28.4 | −5 | 32.4 | +8 | −0.47 | −3.1 |
| 30 | 0.2 | 10.0 | 25.5 | −15 | 23.6 | −21 | −0.34 | −6.1 |
| 30 | 0.5 | 10.0 | 21.7 | −28 | 19.6 | −35 | −0.22 | −7.0 |
| 30 | 1.0 | 10.0 | 22.0 | −27 | 19.3 | −36 | −0.29 | −9.1 |
| 30 | 5.0 | 10.0 | 28.4 | −5 | 33.5 | +12 | −0.90 | −7.7 |
| 60 | 0.2 | 1.0 | 52.9 | −12 | 54.9 | −8 | 0.33 | 3.3 |
| 60 | 0.5 | 1.0 | 51.1 | −15 | 53.7 | −10 | 0.36 | 4.6 |
| 60 | 1.0 | 1.0 | 55.7 | −7 | 59.7 | −0.5 | 3.47 | 13.0 |
| 60 | 5.0 | 1.0 | 59.2 | −1 | 67.5 | +12 | −3.52 | −30.0 |
| 60 | 0.2 | 4.0 | 50.9 | −15 | 52.5 | −12 | 0.18 | 25.0 |
| 60 | 0.5 | 4.0 | 43.2 | −28 | 44.4 | −26 | 0.07 | 2.0 |
| 60 | 1.0 | 4.0 | 38.5 | −36 | 39.6 | −34 | 0.06 | 2.0 |
| 60 | 5.0 | 4.0 | 59.8 | −0.3 | 72.2 | +20 | −8.10 | −83.0 |
| 60 | 0.2 | 10.0 | 50.5 | −16 | 52.0 | −13 | 0.18 | 2.7 |
| 60 | 0.5 | 10.0 | 41.4 | −31 | 42.2 | −30 | 0.03 | 1.0 |
| 60 | 1.0 | 10.0 | 33.2 | −45 | 33.1 | −45 | 0.00 | 0.0 |
| 60 | 5.0 | 10.0 | 57.3 | −4 | 67.2 | +12 | −1.02 | −8.4 |
| 120 | 0.2 | 1.0 | 103.0 | −14 | 115.1 | −4 | 1.34 | 12.0 |
| 120 | 0.5 | 1.0 | 91.3 | −24 | 100.7 | −16 | 0.41 | 8.2 |
| 120 | 1.0 | 1.0 | 87.6 | −27 | 96.1 | −20 | 0.30 | 7.1 |
| 120 | 5.0 | 1.0 | 119.7 | 0 | 143.1 | +19 | −19.4 | −18.5 |
| 120 | 0.2 | 4.0 | 101.0 | −16 | 112.6 | −6 | 0.98 | 10.9 |
| 120 | 0.5 | 4.0 | 83.2 | −31 | 90.8 | −24 | 0.26 | 7.0 |
| 120 | 1.0 | 4.0 | 67.1 | −44 | 71.8 | −40 | 0.10 | 4.0 |
| 120 | 5.0 | 4.0 | 86.2 | −28 | 89.5 | −25 | 0.11 | 3.0 |
| 120 | 0.2 | 10.0 | 100.5 | −16 | 112.0 | −7 | 0.90 | 10.2 |
| 120 | 0.5 | 10.0 | 81.4 | −32 | 88.7 | −26 | 0.21 | 6.0 |
| 120 | 1.0 | 10.0 | 62.9 | −48 | 66.8 | −44 | 0.09 | 4.0 |
| 120 | 5.0 | 10.0 | 41.5 | −65 | 40.7 | −66 | −0.02 | −1.0 |

*Resulting from calculations using and not using three-point smoothing. The values of (T′) and $(\Delta t)(S_e)$ are to be compared.

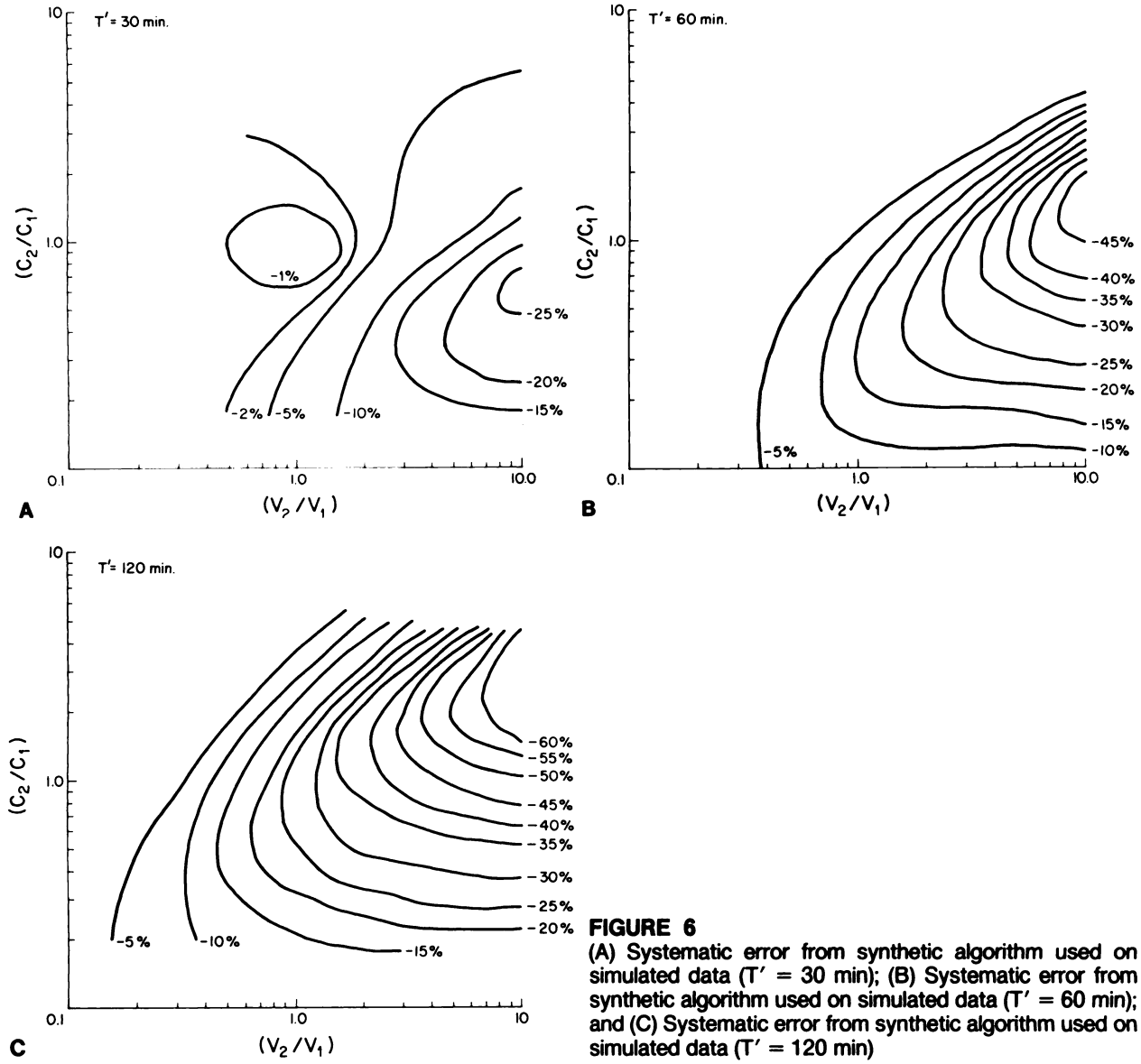


**FIGURE 6**
(A) Systematic error from synthetic algorithm used on simulated data (T′ = 30 min); (B) Systematic error from synthetic algorithm used on simulated data (T′ = 60 min); and (C) Systematic error from synthetic algorithm used on simulated data (T′ = 120 min)

due to a combination of subject variability and uncertainties introduced by the experimental procedure for extracting plasma samples. The resulting noisy simulated input data frequently manifest large deviations from their noiseless counterparts.

Some preliminary experiments with applying our algorithm to these noisy data soon showed us that some smoothing would be desirable in at least some cases to obtain reasonable values for the steady state asymptote [(Δt) ($S_c$)]. However, as previously pointed out, applying a smoothing function is not without its hazards. We chose a simple three-point smoothing algorithm. The weighting among each triplet of points, centered about each given input data point, was (1:2:1). This weighted smoothing was applied to each input data point before the interpolation step, an exception being made for the leading input point (t = 10 min). Typical results showing the systematic error effects introduced by smoothing appear in Table 2. These cases consisted of application of this smoothing procedure to noiseless data. The results indicate that all the consequent equilibrium values [(Δt) ($S_c$)] were shifted somewhat. Generally these shifts were toward larger equilibrium values than those obtained without smoothing, although there were some notable exceptions [e.g., the cases having T′ = 30 min in Table 2]. Even for these exceptional cases, the relative size of the shift was greater when smoothing was applied to more fully sampled data than to those sampled less completely.

These general trends are consistent with intuition. The smoothed curves decay less rapidly than the actual data. We associate this behavior with the fact that the former have less curvature than the latter, indicating that they have been subject to gratuitous "unbending" by the smoothing step. Since the decay of activity then appears to be less rapid in the smoothed data, the

clearance appears to be less than it actually is, producing a consequent increase in the value of $[(\Delta t)\ (S_c)]$ in the calculations, which use smoothed data. Although this systematic distortion has the opposite sense for the ($T'$ = 30 min) simulations than for the ($T'$ = 60 and 120 min), in all cases it is relatively larger for data which are originally more curved than straight. In the extreme, when our smoothing algorithm is applied to straight line data, the line should remain unchanged. Consequently, we expect greater percentage change in the steady state values resulting from smoothing data having greater curvature than those with less. And it is the more completely sampled cases which manifest the curved character of the complete exponential decay function, as compared with the less sampled cases which manifest only the initial, linear part of the exponential.

These observations, although reassuring, do not contribute much from the practical standpoint to an assessment of the quantitative risks of systematic error from smoothing in different particular cases. Moreover since the point of smoothing is to suppress random fluctuations which compromise the certainty in the resultant steady-state value, we require a risk-benefit analysis. For this purpose, we derived two figures of merit in terms of which the advantage of the smoothing could be evaluated.

The first of these we call comparative advantage:

$$CA = (|E_n| - |E_s|)/\sqrt{(|E_n|\ |E_s|)},$$

where, in general $E = [(S_c)\ (\Delta t) - T']/T'$

and in particular $E_s$ and $E_n$ are the (fractional) errors experienced in the asymptote by applying the superposition algorithm to a given simulation function *with* ($E_s$) and *without* ($E_n$) the smoothing, respectively. CA is a dimensionless quantity. It will be negative if the results are worse with smoothing than without. Also notice that CA is inherently large when *either* error is very small, reflecting heavy advantage, or disadvantage, to the use of smoothing in either case.

The second figure of merit, absolute advantage, is simply related to CA:

$$AA = CA * (|E_n| + |E_s|)/2$$

$$AA = (|E_n|^2 - |E_s|^2)/(2*\sqrt{(|E_n|\ |E_s|)}).$$

AA is CA referred to a scale reflecting the actual size of the systematic error caused by the computation process. Not only do these advantage values permit you to calibrate the systematic errors, but they permit you to evaluate the comparative risk-benefits of smoothing.

After the systematic effects of smoothing, we evaluated the random effects of noise by application of our algorithm to various sets of simulated input data, both with and without noise. The results of these tests appear in Table 3. The noisy data used were prepared and tested in sets. For any given choice of simulation function, each associated set uses at least three independent, random realizations for each noise level. The simple average of all the asymptote results from a given set was then compared with the target value, $T'$, in assessing the error and figures of merit.

Table 3 provides some useful rules of thumb for estimating the likely precision in clearance values computed by our method. First, the precision in the determination of the steady state value $[S_c]$ (hence of the clearance rate) depends upon the relative amount of noise present in the data. However, this dependence is

**TABLE 3**
**RMS Fractional Random Error for Clearance Values Extracted from Selected Simulated Data Sets***

| $T'$ (min) | $(C_2/C_1)$ | $(V_2/V_1)$ | % Systematic error | % Random error with Noise at 10% | % Random error with Noise at 20% |
|---|---|---|---|---|---|
| 30 | 0.2 | 1.0 | −12 | 2.1 | 5.9 |
| 30 | 0.5 | 1.0 | −4 | 3.4 | 19.2 |
| 30 | 1.0 | 1.0 | +1 | 6.8 | 18.7 |
| 30 | 5.0 | 1.0 | 0 | 0.6 | 21.4 |
| 30 | 0.2 | 4.0 | −20 | 3.5 | 11.8 |
| 30 | 0.5 | 4.0 | −25 | 1.8 | 12.0 |
| 30 | 1.0 | 4.0 | −10 | 72 | 2,600 |
| 30 | 5.0 | 4.0 | +8 | 88 | 64 |
| 30 | 0.2 | 10.0 | −21 | 1.7 | 0.4 |
| 30 | 0.5 | 10.0 | −35 | 1.0 | 7.0 |
| 30 | 1.0 | 10.0 | −36 | 9.7 | 92 |
| 30 | 5.0 | 10.0 | +12 | 590 | 6,900 |
| 60 | 0.2 | 1.0 | −8 | 3.7 | 8.4 |
| 60 | 0.5 | 1.0 | −10 | 2.5 | 4.3 |
| 60 | 1.0 | 1.0 | −0.5 | 21.9 | 100 |
| 60 | 5.0 | 1.0 | +12 | 15.3 | 115 |
| 60 | 0.2 | 4.0 | −12 | 5.5 | 7.2 |
| 60 | 0.5 | 4.0 | −26 | 7.7 | 22.9 |
| 60 | 1.0 | 4.0 | −34 | 0.5 | 9.2 |
| 60 | 5.0 | 4.0 | +20 | 20.3 | 110 |
| 60 | 0.2 | 10.0 | −13 | 8.1 | 12.6 |
| 60 | 0.5 | 10.0 | −30 | 4.5 | 8.1 |
| 60 | 1.0 | 10.0 | −45 | 1.9 | 18.5 |
| 60 | 5.0 | 10.0 | +12 | 30.2 | 136 |
| 120 | 0.2 | 1.0 | −4 | 12.7 | 32.8 |
| 120 | 0.5 | 1.0 | −16 | 21.7 | 57 |
| 120 | 1.0 | 1.0 | −20 | 12.6 | 18.7 |
| 120 | 5.0 | 1.0 | +19 | 129 | 79 |
| 120 | 0.2 | 4.0 | −6 | 11.8 | 77 |
| 120 | 0.5 | 4.0 | −24 | 13.1 | 144 |
| 120 | 1.0 | 4.0 | −40 | 6 | 40 |
| 120 | 5.0 | 4.0 | −25 | 456 | 103 |
| 120 | 0.2 | 10.0 | −7 | 22.5 | 19 |
| 120 | 0.5 | 10.0 | −26 | 22.4 | 56 |
| 120 | 1.0 | 10.0 | −44 | 4.7 | 18.7 |
| 120 | 5.0 | 10.0 | −66 | 32 | 89 |

*Containing different levels of added noise using smooth, compared with systematic error.

not a linear relation. Systematic errors aside, the uncertainty in results for many cases having 10% relative noise in their data points is about 5–10% with respect to the mean clearance rates obtained. But the analogous uncertainties for those same input functions having 20% relative noise is 15–30%, *more* that twice as much.

Second, for simulated data containing effects of a second compartment, the superposition technique usually biases the results toward *lower* steady state values, hence *higher* computed clearance rates. For most test cases examined, this effect is somewhat ameliorated by an opposite bias of the smoothing. The exceptions for smoothing are the cases of completely sampled data; in our simulations, where we always used sampling time span (T = 120 min), these are the cases where (T′ = 30 min). However, also for these exceptions, the effects of noise were relatively small where the second-compartment volume and permeability are moderate. This suggests that more thorough sampling, if possible clinically, might be a more suitable alternative than smoothing, at least for moderately noisy data.

Third, there are number of cases where noise is especially pathological to our method. These cases with unacceptable lack of precision (random error >100%) most frequently are associated with the combination of large extracellular volume and high second-compartment permeability. The subset of these cases most vulnerable to high noise appeared, again as with biases from smoothing, to be the most completely sampled cases. This fact suggests that, for very noisy data in these particular physiological situations, *less* complete sampling may give more reliable results. This is counterintuitive and somewhat disturbing.

## SUMMARY

We have mentioned that the underlying principle of our calculation of clearance is that of superposition. The calculation uses experimental data, in the form of the plasma activity response to a single-shot injection, to formulate a sum graph; this is the single-shot graph repeatedly shifted and added to itself. This superposition process simulates the response to a continuous infusion of the radioactive substituent. In addition, we augment the superposition sum by modifying its first component, making that proportionately larger. This mathematical modification of the initial component corresponds to the physical modification of the continuous infusion process by means of a "priming" injection. The mathematical rationale for this modification is the achievement of steady state, asymptotic behavior of the resultant plasma response within the sampling time span. This corresponds to the physiological rationale for the procedure of equilibrating the tracer substituent among all the fluid compartments which are accessible to it.

## APPENDIX

### Design for Convolution Program Which uses Impulse Synthesis to Evaluate Clearance

Input experimental data values: sample activity versus corresponding time.

Do an extrapolation of log (data) back to the time = 0 point.

Do an interpolation of log (data) to a linear, piece-wise continuous curve between adjacent pairs of data points.

Repeatedly

- Input adjustable parameters and options which specify the convolution algorithm used to evaluate the synthetic response to a simulated, continuous infusion. [Δt, no/smoothing, priming injection];
- Compute the synthesis superposition using the selected priming injection; evaluate the terminal slope, and the terminal sum;
- Compute another synthesis superposition using *twice* the selected priming injection; calculate second values for "terminal" slope and the terminal sum;
- Make a linear extrapolation, using the pairs of terminal slope and sum values just calculated, to estimate a terminal sum value (superposition asymptote) for the case of zero terminal slope; and
- Use the given relation between superposition asymptote and timeshift increment to obtain an estimate for the clearance value;

until you are satisfied and wish to quit.

## ACKNOWLEDGMENTS

The authors gratefully acknowledge the contributions of Dr. John McAfee to the substance of this manuscript and of Ms. Carol Westfall for secretarial assistance.

This work was supported in part by PHS Grant No. AM33357 awarded by the National Institute of Arthritis, Diabetes, and Digestive and Kidney Diseases, DHHS.

## REFERENCES

1. Wooten R, Sanderson PJ: Forecasting antibiotic regimes using impulse analysis. *J Antimicrobiol Chemotherapy* 6:73–81, 1980
2. Veall N and Gibbs GP: The accurate determination of tracer clearance rates and equilibrium distribution volumes from single injection plasma measurements using numerical analysis. In *Radionuclides in Nephrology*, Joekes AM, Constable AR, Brown NJG, et al. eds. New York, Grune and Stratton, 1982, pp 125–130
3. Groth S, Aasted M: $^{15}$Cr-EDTA clearance determined by one plasma sample. *Clinical Physiol* 1:417–425, 1981
4. Saperstein LA, Vidt DG, Mandel MJ, et al: Volumes

of distribution and clearances of intravenously injected creatinine in the dog. *Am J Physiol* 181:330–336, 1955
5. Jacobsson L: A method for the calculation of renal clearance based on a single plasma sample. *Clin Physiol* 3:297–305, 1983
6. Chantler C, Garnett ES, Parson V, et al: Glomerular filtration rate measurement in man by the single-injection method using $^{15}$Cr-EDTA. *Clin Sci* 37:169–180, 1969
7. Brochner-Mortensen J: Routine methods and their reliability for assessment of glomerular filtration rate in adults. *Dan Med Bull* 25:181–202, 1978
8. Veall N, Vetter H: Radioisotope techniques. In *Clinical Research and Diagnosis*, Chapter 10. Buttersworth, London, 1958